Available online at www.sciencedirect.com
ScienceDirect
Journal of Power Sources 166 (2007) 337–342
JOURNAL OF POWER SOURCES
www.elsevier.com/locate/jpowsour

Short communication

Ni–YSZ gradient anodes for anode-supported SOFCs

Jiangrong Kong, Kening Sun *, Derui Zhou, Naiqing Zhang, Ju Mu, Jinshuo Qiao

Department of Applied Chemistry, Harbin Institute of Technology, No. 92, West Da-Zhi Street, Harbin, Heilongjiang 150001, PR China

Received 5 November 2006; received in revised form 17 December 2006; accepted 20 December 2006
Available online 30 December 2006

Abstract

A novel multilayer Ni–YSZ anode structure, which had a gradient in particle size and Ni content, was introduced in this paper. This gradient anode was co-fabricated with electrolyte by a symmetrical uniaxial die-pressing method. The anode functional layer (AFL) was developed to several sub-layers. The influences of different composition and various thickness of the AFL were investigated. The thickness of anode effective electrochemical reaction zone was ascertained to about 40–50 μm. A unit cell with gradient in both particle size and Ni content demonstrated a maximum power density of 467.14 mW cm^{-2}. EIS result demonstrated that the surface dissociation/diffusion step is easier than charge-transfer reaction, which indicated that the microstructure of the anode, especially anode functional layer, was well fabricated and the distribution of the two phases was homogeneous thus the interfacial resistance was dampened.

Keywords: Solid oxide fuel cell (SOFC); Gradient anode; Anode functional layer (AFL); Ni–YSZ cermet; Microstructure; Cell performance

1. Introduction

Lowering the working temperature of solid oxide fuel cells (SOFCs) would be of benefit because it extends durability of SOFC cells, expands applicable kinds of materials and elevates SOFC cost performance. Reducing thickness of solid electrolyte is one of the most effective strategies to keep low ohmic loss derived from an electrolyte at reducing temperatures [1]. In recent years, the anode-supported design has been extensively investigated [2,3].

Many SOFC anode reports have been concerned on the preparation and characteristics of various anode materials [4–6]. The performance, such as electrochemical and physical properties of electrodes in SOFCs, strongly depends on the morphology and chemical composition of the electrodes [7,8]. However, few works have been reported on anodic structure development.

A two-layered anode structure for the anode-supported solid oxide fuel cell has been proposed by Virkar et al. [9] in an attempt to minimize both the concentration and activation polarizations. The microstructure of the interlayer was made finer than that of outer support layer in terms of volume percent porosity, pore size, and its distribution. Based on their work, we proposed a novel multilayer anode structure, which had a gradient in particle size and Ni content and therefore a gradient of porosity, electrical conductivity, and thermal expansion coefficient. The anode functional layer (AFL), which was named "interlayer" in Virkar's work, was developed into several sub-layers.

High performance anode needs a wealth of three phase boundaries (TPBs), where fuel gas and an oxygen ion can contact along electric conduction paths, because the conversion occurs at TPBs inside an anode [10]. The anode functional layer, which was close to the electrolyte proximately, was the area where most of the electrocatalysis related to hydrogen oxidation occurs. The optimization of AFL structure could enlarge TPB area thus increasing cell performance. In addition, graded structure along thickness direction in terms of both Ni content and Ni/YSZ particle size ratio is quite effective in either transference of charge and gas or tailoring the thermal expansion coefficient [11].

In this article, we took effort to obtain improved microstructure including larger TPB composed of Ni and YSZ grains in the AFL for the achievement of high-performance SOFC anode.

2. Experimental

2.1. Cell fabrication

A typical half-cell used in the present work consisted of the following three layers. (a) Porous Ni + YSZ anode support. (b)

* Corresponding author. Tel.: +86 451 8641 2153; fax: +86 451 8641 2153.
E-mail address: sunkn_skn@yahoo.com.cn (K. Sun).

0378-7753/$ – see front matter © 2007 Elsevier B.V. All rights reserved.
doi:10.1016/j.jpowsour.2006.12.042

Porous Ni + YSZ anode functional layer. (c) Dense YSZ electrolyte. The AFL was split into several sub-layers to develop the microstructure.

The anode/electrolyte green discs were symmetrical uniaxially die-pressed. AR grade NiO powder was purchased from China Medicine (Group) Shanghai Chemical Reagent Corporation. YSZ powder was purchased from China building Materials Academy. The starting powders were sifted to different particle sizes after the pretreatments included ball-milling, preheat, and ultrasonic dispersion. Without specially indicated, the powder sizes were 0.8–5 and 0.5–3 μm for YSZ and NiO, respectively. The green powders were mixed in right ratio and ball milled for 24 h to ensure good dispersion. Then they were mixed with organic binder and pore former, if needed, in mortar. Every layers of the sample were fabricated well proportioned by bestrewing the ceramic powder into the die and followed by a prepressing procedure. After all the layers were filled, the granules of NiO–YSZ mixture were compacted and uniaxially pressed into pellets of 20 mm diameter at 300 MPa. The filling sequence of the layers was illustrated in Fig. 1. Symmetrical mode was employed to reduce the stress during co-sintering of the anode/electrolyte composite ceramic.

The anode/electrolyte composite ceramic was co-sintered at 1500 °C for 5 h in air and then platinum paste was burned on the electrolyte surface as a cathode at 850 °C for 1 h. Pt was used as cathode because of its favorable catalysis of O_2 reduction. LSM material is the most used cathode material, but the preparation process of LSM cathode is more complicated than Pt paste cathode used in our study. This paper concerned the anode performances, so we chose Pt cathode instead of LSM cathode.

2.2. Cell testing

The scheme of the electrochemical testing apparatus was illustrated in Fig. 2. The samples were sealed by a glass-ceramic sealant. Silver wires were used as current collectors and adhered by silver paste on the Pt paste cathode and the anode substrate, respectively. Arbin fuel cell testing system was employed to measure current–voltage curves of the unit cells. The discharge tests were performed at 800 °C using 60 sccm flow rate H_2 fuel with a humidity of approximately 3%. NiO–YSZ composite ceramic was first reduced into Ni–YSZ cermet by H_2 at SOFC working temperature 800 °C. The tests characterized the open circuit voltage (OCV) of the cell and ensure that there was little cross-leak or electronic conductivity in the electrolyte and that there is a good seal between components.

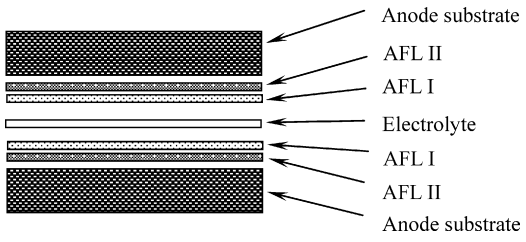

Fig. 1. Scheme of symmetrical uniaxially die-pressing.

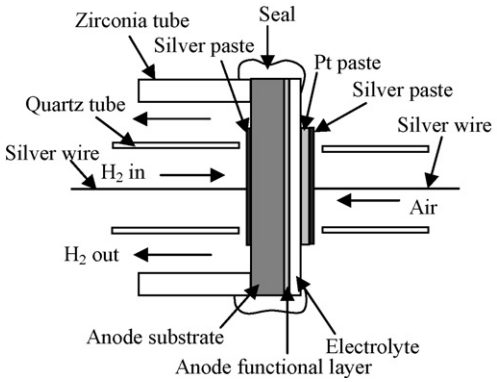

Fig. 2. Schematic of the unit cell testing arrangement.

2.3. Microstructure characterization

After testing, some of the cells were fractured and cross-sections were examined under a Hitachi S-570 scanning electron microscope (SEM).

2.4. Electrochemical impedance spectroscopy (EIS)

A PARSTAT 2273 advanced electrochemical system was employed for EIS measurement. The Electrochemical impedance measurements were made over the frequency range of 1 Hz–100 kHz with an applied amplitude of 5 mV under open-circuit at 800 °C. The measured spectra were fitted to the equivalent circuit by using the nonlinear least square fitting software, ZSimpWin, developed by Bruno Yeum.

3. Results and discussion

3.1. Influence of anode functional layers thickness on cell performances

The influence of AFL with different thickness on cell performances was studied by fixing the compositions of the anode substrate and the electrolyte. The anode substrates consisted of 70 wt% NiO and 30 wt% YSZ. The thicknesses of anode substrates and the YSZ electrolyte membranes were fixed at about 600 and 30 μm, respectively. Four types of unit cells A, B, C, and D were prepared with different AFLs, see in Table 1. There was an incremental decrease in the total AFL thicknesses (the summation of the thicknesses of AFL I and AFL II) of the unit cells. The discharge performances of the unit cells A–D were

Table 1
Components in unit cells with different thicknesses of anode functional layers

Component	NiO:YSZ (wt%)	Thickness (μm)			
		A	B	C	D
Electrolyte	–	30	30	30	30
AFL I	50:50	60	40	20	20
AFL II	60:40	60	40	40	20
Anode substrate	70:30	600	600	600	600
Maximum power density (mW cm^{-2})		171.45	205.08	290.96	374.77

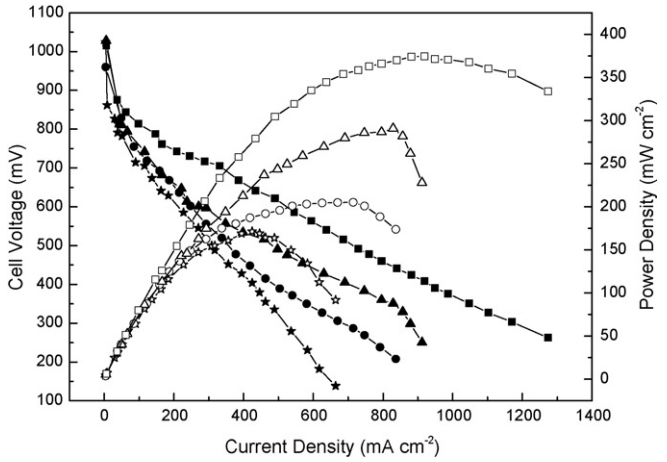

Fig. 3. *I–V* curves and current–power density curves of SOFC unit cells with different AFL thickness (★: cell A; ●: cell B; ▲: cell C; ■: cell D).

given in Fig. 3. The 30-μm electrolytes were thick enough to prevent gas permeation, thus ensuring high OCV in discharging tests. With the decreasing of the AFL thickness, the cell performance increased. It was concluded from the results that the thickness of the anode effective electrochemical reaction zone (ERZ) which materialized as the AFL is about 40–50 μm. We are aware that Ni acts as a catalyst at the SOFC anode. The Ni proportion in cermet anode directly determines electrocatalytic activity of the electrode [12]. In this study, the weight ratio of NiO:YSZ of AFL I was 50:50. The thickness of AFL I of cell A is about 60 μm. That is to say, the ERZ of cell A consists only Ni–YSZ cermet of low Ni ratio. For cell D, its ERZ could include both AFL I and AFL II. Ni ratio in AFL II was higher than that in AFL I. The total Ni ratio increased, thereby gaining improved cell performance.

3.2. Optimization of AFL structures

3.2.1. The influence of different AFL compositions on cell performance

The compositions of the anode substrate and the electrolyte were still fixed to study the optimization of AFL structures on cell performances. The components and proportions of the anode substrates and the electrolytes were the same with those in Section 3.1. Cell E was prepared as a single AFL structure. The AFL of cell E consisted of 60 wt% NiO and 40 wt% YSZ and the thickness was about 60 μm. Cell C was prepared as a bi-AFL structure, which was already described in Section 3.1. The AFL structures of cells C and E were described in Table 2. The total thickness of cell C's AFL was 60 μm, which was the same with that of cell E. The total Ni ratio in cell C's AFL was lower than that in cell E's, but the maximum power density of cell C was higher than that of cell E. The reduction of NiO to Ni leaves some porosity in the bulk, therefore NiO–YSZ composite ceramic could convert into porous Ni–YSZ cermet. The higher NiO content is, the more pronounced the porosity of the cermet could be, on precondition of no pore former added. Gradient NiO contents consequentially bring gradient porosity that could be in favor of the transfer of fuel and exhaust gas and enlarged

Table 2
Thicknesses of components in unit cells C and E

Component	NiO:YSZ (wt%)	Thickness (μm)	
		C	E
Electrolyte	–	30	30
AFL I	50:50	20	–
AFL II	60:40	40	60
Anode substrate	70:30	600	600
Maximum power density (mW cm^{-2})		290.96	253.48

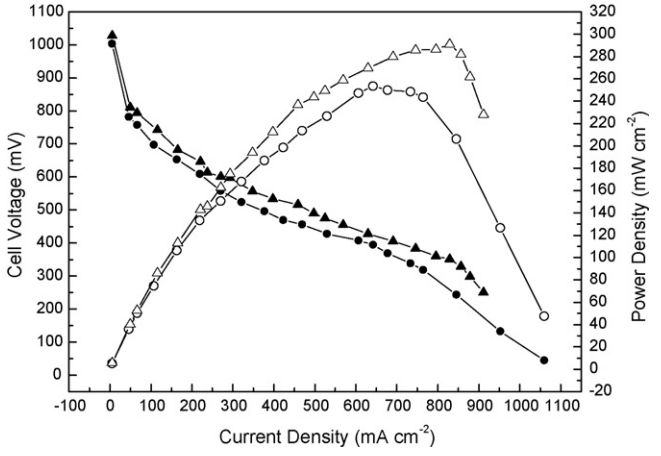

Fig. 4. *I–V* curves and current–power density curves of SOFC unit cells with different AFL structures (▲: cell C; ●: cell E).

TPB area. The discharge performances of cells C and E were schemed in Fig. 4. The maximum power density of cell C was higher, which was attributing to the better AFL structure that offering more TPB area.

The discharge results of the unit cells revealed that the gradient structure AFL showed advanced performance. That would be attributed to the more contribution of gradient structure in triple phase boundary's formation and gas transference.

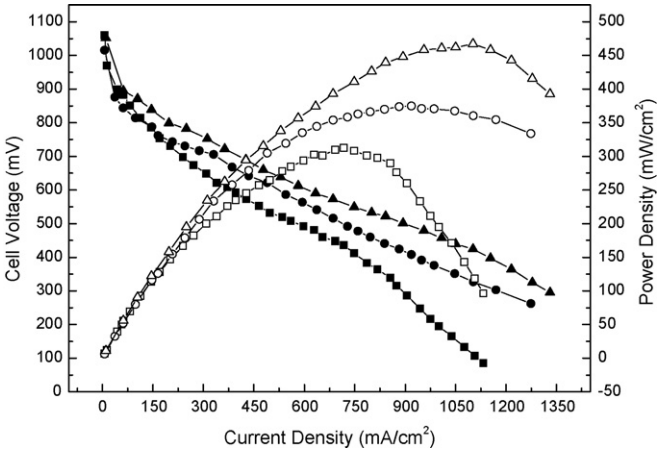

Fig. 5. *I–V* curves and current–power density curves of SOFC unit cells with different AFL structures (■: cell F; ●: cell D; ▲: cell G).

3.2.2. The influence of AFL particle sizes on cell performance

The AFL structure was fabricated more detailed in particle size selection. A group of unit cells were fabricated and their performances were compared with each other from the viewpoint of AFL structure changes. Three kinds of unit cells were made with fixed components and proportions of their anode substrates and electrolytes, which was illustrated in Table 3. Cell F was a single AFL structure, whilst cell D and cell G were bi-AFL structures. If cell F and cell D were taken out and compared with each other, the result confirmed the conclusion in Section 3.2.1, that gradient structure AFL was better than sin-

Table 3
Components in unit cells with different compositions and particle sizes of anode functional layers (a: YSZ 0.89 μm; b: NiO 0.53 μm, YSZ 1.42 μm; c: NiO 2.85 μm, YSZ 3.87 μm)

Component	NiO:YSZ (wt%)	Thickness (μm)		
		F	D	G
Electrolyte	–	30	30	30 (a)
AFL I	50:50	–	20	20 (b)
AFL II	60:40	40	20	20 (b)
Anode substrate	70:30	600	600	600 (c)
Maximum power density ($mW\,cm^{-2}$)		301.1	374.77	467.14

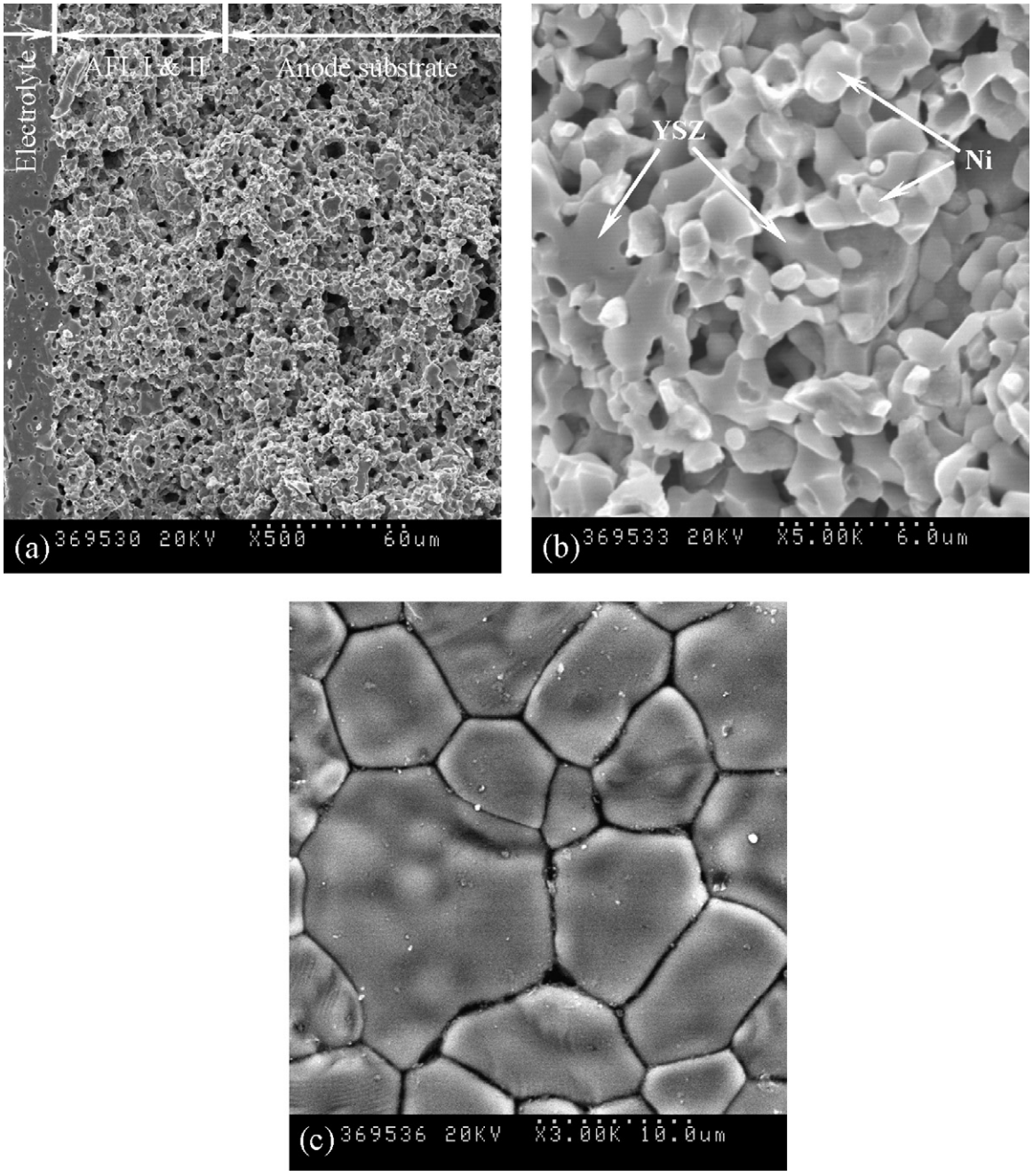

Fig. 6. Scanning electron micrographs of anode-supported thin-film YSZ electrolyte cell: (a) cross-section of electrolyte/anode; (b) magnified image of anode functional layer after test; (c) surface of YSZ electrolyte.

Table 4
Electrochemical characteristics of cell G at 800 °C in H_2–H_2O

Symbol	L (H cm^2)	R_s (Ω cm^2)	Q_1 (F cm^{-2})	n	R_1 (Ω cm^2)	Q_2 (Ω^{-1} cm^{-2} s^{-n})	n	R_2 (Ω cm^2)
Value	6.795E−8	0.225	0.003659	0.6885	0.209	0.13514	0.853	0.064

gle AFL structure. Besides compositions, the particle sizes of Ni and YSZ in components of cell G were carefully regulated. A 600-μm thick anode substrate (70 wt% NiO 2.85 μm, YSZ: 3.87 μm), a 20-μm thick AFL II (60 wt% NiO 0.53 μm, YSZ: 1.42 μm) and a 20-μm thick AFL I (50 wt% NiO 0.53 μm, YSZ: 1.42 μm) composed cell G's anode. The electrolyte was fabricated adopting YSZ powder of 0.89 μm. The multilayer AFL had a gradient in particle size and Ni content and therefore a gradient of porosity, electrical conductivity, and thermal expansion coefficient. Discharge performances of the three unit cells were showed in Fig. 5. From the results it can be concluded that the finer the AFL structure is, the larger the TPB area would be, and the better the cell performance could be.

3.3. Microstructure

The SEM graph of the cross-section of a fresh fractured unit cell after test was surveyed, which was showed in Fig. 6(a). The YSZ electrolyte on the left is dense except for some closed holes. The anode functional layers are proximate to that of an electrolyte. It has small grain sizes, sufficient porosity and very even distribution of the nickel phase, the YSZ ceramic phase and the pores respectively. The interface of AFL I and AFL II cannot be observed clearly, because of their close compositions. The microstructure of anode substrate is coarser and more porous than that of AFL. Fig. 6(b) shows the magnified microstructure of AFL in 5k times. The smooth gray phase is YSZ and the dispersed grains are Ni. YSZ phase forms well-proportioned ceramic skeleton and nickel grains connected with each other. The dimensional structure is clear and does not collapse after testing. Fig. 6(c) shows the surface photograph of YSZ electrolyte. The grains of YSZ electrolyte abut upon each other and leave little interstice thus the electrolyte could be gastight macroscopically.

3.4. Electrochemical impedance performance

The electrochemical behaviors of the unit cells were investigated by EIS measurement under open circuit conditions. The spectra of the all the unit cells were similar in shape. Fig. 7 showed EIS response and its equivalent circuit of cell G under open-circuit in fuel cell operating condition. The solid line in Fig. 7 is the fitted result of the ZSimpWin program.

The symbols were denoted as follows: R_s is the ohmic resistance of electrolyte and lead wires, CPE (Q) the constant phase element, R_1 and R_2 the electrode resistances, and L is the inductance of lead wires. The impedance diagram is composed of two semicircles referred to as HF (for high frequency) and MF (for middle frequency). The observation of two clearly separated arcs in the frequency domain indicates that H_2 oxidation at Ni–YSZ

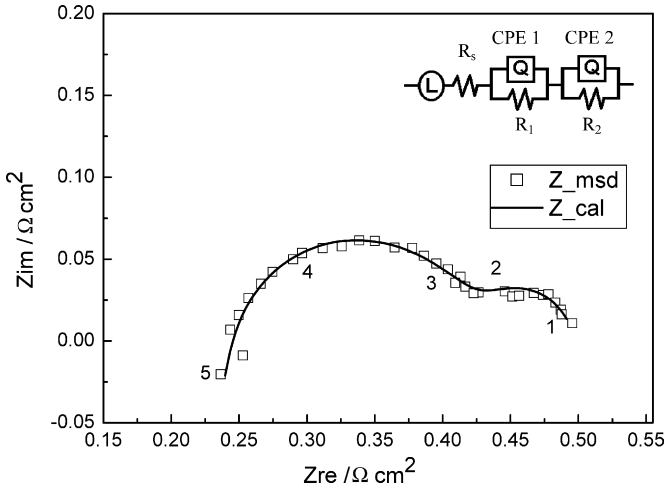

Fig. 7. EIS response at open circuit voltage tested at 800 °C for anode-supported solid oxide fuel cells with thin-film YSZ electrolyte and with Pt cathode. Numbers indicate frequencies in powers of 10 Hz.

cermet electrodes is controlled by at least two electrode processes in series. The middle frequency arc is associated with a slow hydrogen dissociative adsorption or a surface diffusion process at the Ni surface (the first electrode process). The process associated with the high frequency arc appears to be related to a charge transfer reaction at the electrode/electrolyte interface (the second electrode process) [13].

The polarization resistance R_p is defined as [14]:

$$R_p = R_1 + R_2 \quad (1)$$

The values of the symbols were illustrated in Table 4. Ohmic resistance R_s was 0.225 Ω cm^2, electrode resistance R_p was the summation of R_1 and R_2, numerically 0.273 Ω cm^2. R_2 is smaller than R_1, which reveals that the effect of charge-transfer reaction appears to be more dominant. In other words, surface dissociation/diffusion step is easier than charge-transfer reaction. This means the microstructure of the anode, especially anode functional layer, was fabricated fine and the distribution of the two phases homogeneous thus reduced the interfacial resistance and then the cell performance could be increased.

4. Conclusion

Gradient anode/electrolyte composite ceramic was fabricated by a symmetrical uniaxially die-pressing method. On the basis of this composite ceramic, unit cells were prepared. The AFL was developed to several sub-layers to optimize the microstructure. Through our research, the thickness of anode effective electrochemical reaction zone was ascertained to about 40–50 μm. Gradient structure AFL was more contributive in triple phase boundary's formation and gas transferring. Further more, the

particle sizes in every sub-layer were controlled during cell fabrication. The unit cell fabricated with both particle size and Ni content controlled displayed a pronounced performance. The cell maximum power density reached 467.14 mW cm^{-2}. EIS result showed that the surface dissociation/diffusion step is easier than charge-transfer reaction, which indicated that the microstructure of the anode, especially anode functional layer, was well fabricated and the distribution of the two phases was homogeneous thus the interfacial resistance was diminished.

Acknowledgements

This work was financially supported by the National Nature Science Foundation of China (No. 90510006) and the National High-tech Research and Development of China (No. 2003AA302440).

References

[1] W.Z. Zhu, S.C. Deevi, Mater. Sci. Eng. A362 (2003) 228–239.
[2] F. Gutierrez-Mora, J.M. Ralph, J.L. Routbort, Solid State Ionics 149 (2002) 177–184.
[3] J.-R. Kong, K.-N. Sun, D.-R. Zhou, Chin. J. Nonferrous Met. S3 (14) (2004) 380–383.
[4] S. Suda, M. Itagaki, E. Node, S. Takahashi, M. Kawano, H. Yoshida, T. Inagaki, J. Eur. Ceram. Soc. 26 (2006) 593–597.
[5] S.P. Jiang, S.H. Chan, J. Mater. Sci. 39 (2004) 4405–4439.
[6] T. Fukui, K. Murata, S. Ohara, H. Abe, M. Naito, K. Nogi, J. Power Sources 125 (2004) 17–21.
[7] J.-H. Lee, J.-W. Heo, D.-S. Lee, J. Kim, G.-H. Kim, H.-W. Lee, H.S. Song, J.-H. Moon, Solid State Ionics 158 (2003) 225–232.
[8] J.-H. Lee, H. Moon, H.-W. Lee, J. Kim, J.-D. Kim, K.-H. Yoon, Solid State Ionics 148 (2002) 15–26.
[9] A.V. Virkar, J. Chen, C.W. Tanner, J.W. Kim, Solid State Ionics 131 (2000) 189–198.
[10] Y. Sunagawa, K. Yamamoto, A. Muramatsu, J. Phys. Chem. B 110 (2006) 6224–6228.
[11] A.C. Muller, D. Herbstritt, E.I. Tifffee, Solid State Ionics 152–153 (2002) 537–542.
[12] H. Koide, Y. Someya, T. Yoshida, T. Maruyama, Solid State Ionics 132 (2000) 253–260.
[13] S.P. Jiang, S.P.S. Badwal, Solid State Ionics 123 (1999) 209–224.
[14] M. Guillodo, P. Vernoux, J. Fouletier, Solid State Ionics 127 (2000) 99–107.